Supplementary Data

Functional Domains of the 50S Subunit Mature Late in the Assembly Process

Ahmad Jomaa[1¥], Nikhil Jain[2¥], Joseph H. Davis[3¥], James R. Williamson[3], Robert A. Britton[2*] and Joaquin Ortega[1*]

[1]Department of Biochemistry and Biomedical Sciences and MG. DeGroote Institute for Infectious Diseases Research, McMaster University, 1280 Main Street West, Hamilton, Ontario, L8S4K1, Canada; [2]Department of Microbiology and Molecular Genetics, Michigan State University, East Lansing, MI 48824, USA; [3]Department of Molecular Biology, Department of Chemistry and The Skaggs Institute for Chemical Biology, The Scripps Research Institute, La Jolla, CA 92037, USA.

This supplement contains:

Supplementary Figures S1 to S12

Supplementary Tables 1 to 3

Supplementary References

SUPPLEMENTARY FIGURES

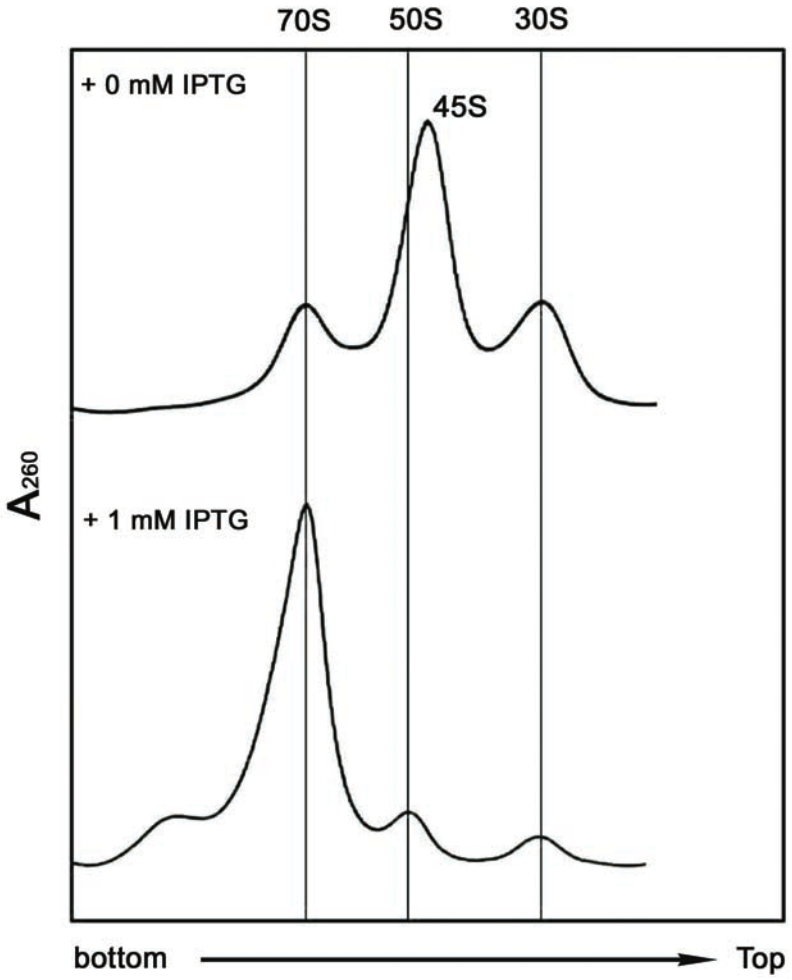

Supplementary Figure S1. Sedimentation profiles from sucrose gradients of ribosomal particles purified from RbgA depleted *B. subtilis* cells. The profiles correspond to cells in which transcription of *rbgA* is under the control of an IPTG inducible P_{spank} promotor (RB301). Cells grown in the presence of the inducer (bottom panel) produce a ribosome profile similar to wild type cells, but absence of the inducer (top panel) caused depletion of RbgA and concomitant accumulation of 45S particles.

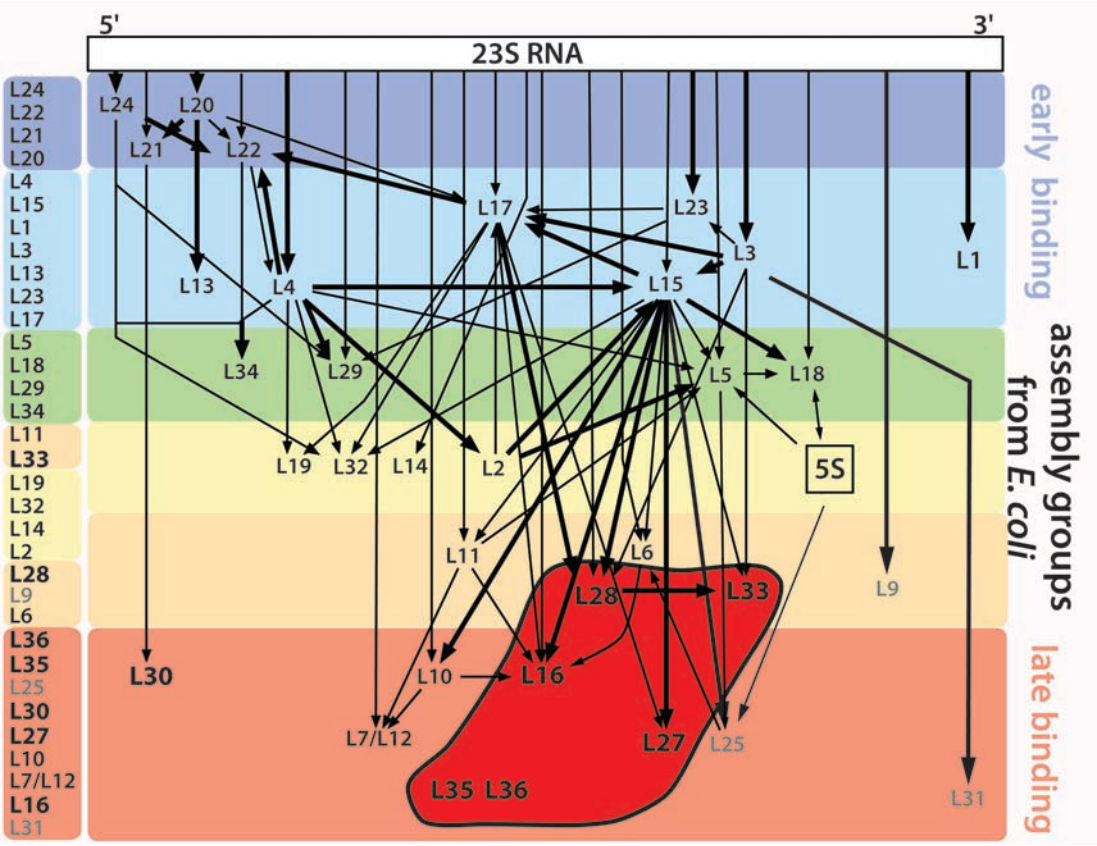

Supplementary Figure S2. Protein complement of the 45S particle purified from RbgA-depleted *B. subtilis* cells. Ribosomal proteins are placed in the *in vivo* assembly map for the 50S subunit. Groups of r-proteins exhibiting similar binding profiles as establish in Chen and Williamson 2013[1] are marked with purple (the earliest-binding proteins), cyan, green, yellow, and red (the latest-binding proteins). The dark red box highlights proteins that are significantly depleted or missing from the 45S particles. Proteins we could not identify in both the 45S particles and 50S subunits from IF2-depleted cells are shown in grey.

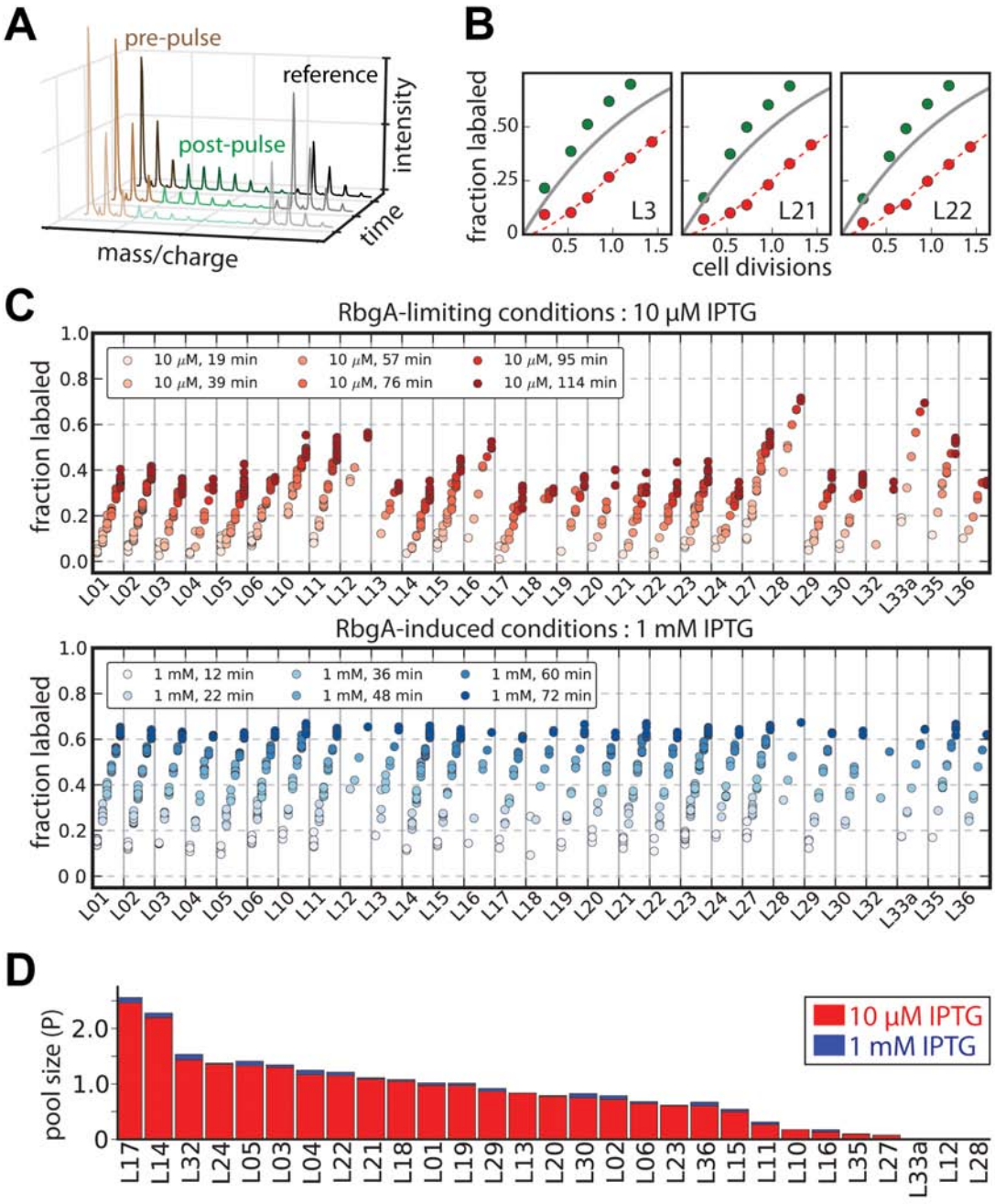

Supplementary Figure S3. Pulse labeling experiments determined that the 45S particle can mature into a complete ribosome. (A) Pulse-labeling isotope distribution. Three isotope distributions are fit for each peptide and each time point. The ^{14}N distribution (brown) is fit to quantify material synthesized before the pulse. The partially-labeled distribution (green) is fit to quantify material synthesized after the pulse. A ^{15}N-labeled reference standard (black) is included to aid in peptide identification. (B) Labeling kinetics of proteins in 45S particles (green) or 70S

particles (red). The maximum labeling rate in the absence of protein turnover is depicted by the solid grey line. Labeling kinetics of 70S particles were fit as described in [2](dashed lines). "Overlabeling" (green) was predicted for an on-pathway intermediate as described in Chen et al. 2012[2]. (C) Label incorporation under RbgA-limiting (top) or RbgA-induced (bottom) conditions. Fraction labeled is calculated as [post-pulse]/[post-pulse + pre-pulse]. Each marker represents a unique measurement of a peptide resulting from a tryptic digest of the parent protein. (D) Stacked bar graph of fit pool size (P). For each protein, the small pools (0-0.1) observed in the presence of 1 mM IPTG (blue) are stacked above the large pools (0-2.47) observed in the presence of 10 μM IPTG (red). Cellular doubling times were 48 and 85 minutes for the RbgA-induced and RbgA-limited conditions respectively.

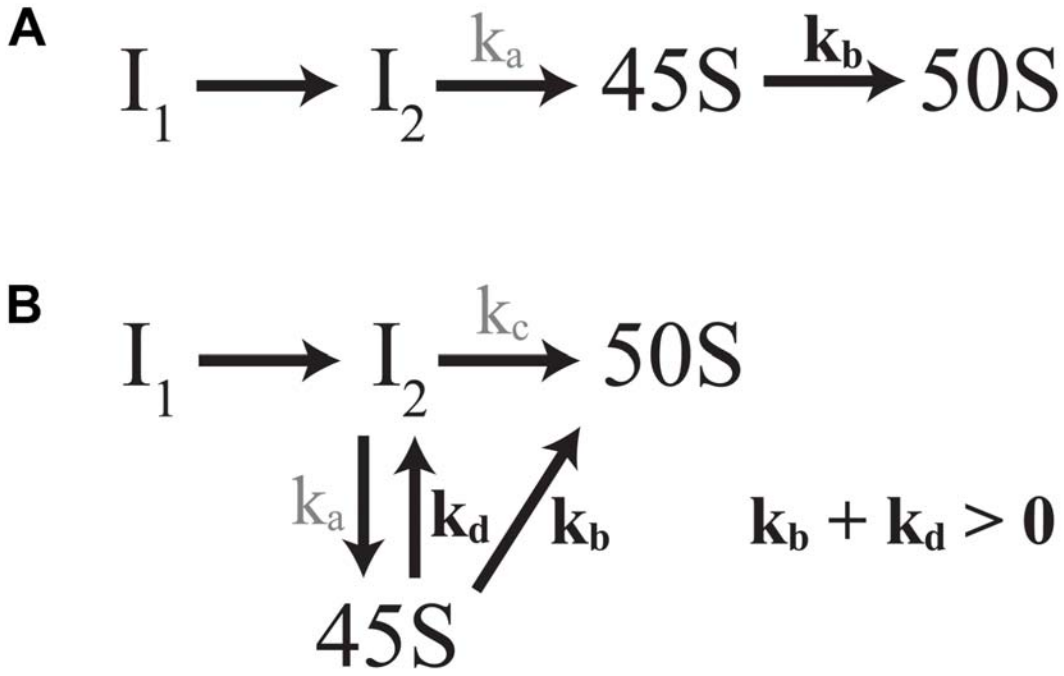

Supplementary Figure S4. Kinetic models of ribosome biogenesis consistent with pulse labeling experiments. (A) A linear pathway. RbgA directly catalyzes the conversion of the 45S particle to a mature 50S subunit by increasing the rate of a slow step late in assembly (k_b, bold). (B) Parallel pathway. I_2 and the 45S can interconvert and each is competent for maturation. RbgA could increase either the k_b or k_d rates (bold). Related variants of this model arise if any of k_b, k_c, or k_d are zero, however, our pulse-labeling results show that either k_b or k_d must be nonzero. For example, if $k_b = 0$, then RbgA accelerates k_d and is effectively rescuing the 45S particle and providing multiple opportunities for the I_2 intermediate to properly mature. Alternatively, if $k_d = 0$, parallel pathways emerge with RbgA accelerating the rate of 45S-to-50S conversion, k_b.

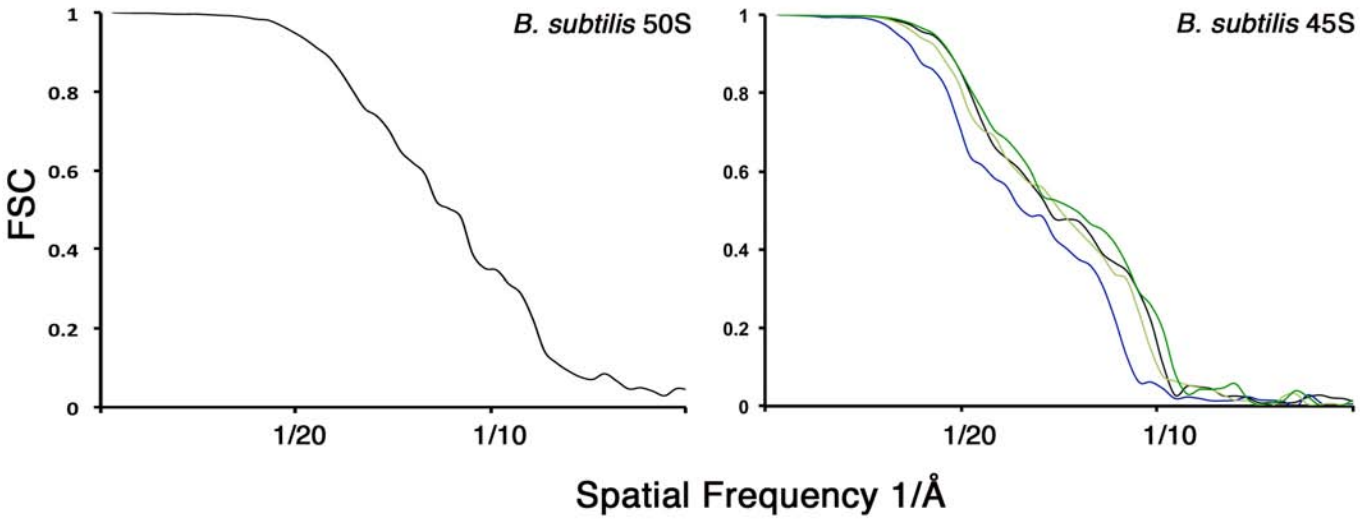

Supplementary Figure S5. Fourier Shell Correlation plots for resolution estimation of the 3D structures of the 50S subunit and 45S particle. Using the the FSC=0.5 criteria the estimated resolution for the 3D reconstruction of the mature 50S subunit was 11 Å. In the case of the 45S particle structures the plots correspond to the cryo-EM reconstructions obtained for the four conformational subpopulations: CL1 (black), CL2 (blue), CL3 (orange) and CL4 (green). The estimated resolution was 13 Å resolution for CL1, CL3 and CL4 and 15 Å resolution for CL2.

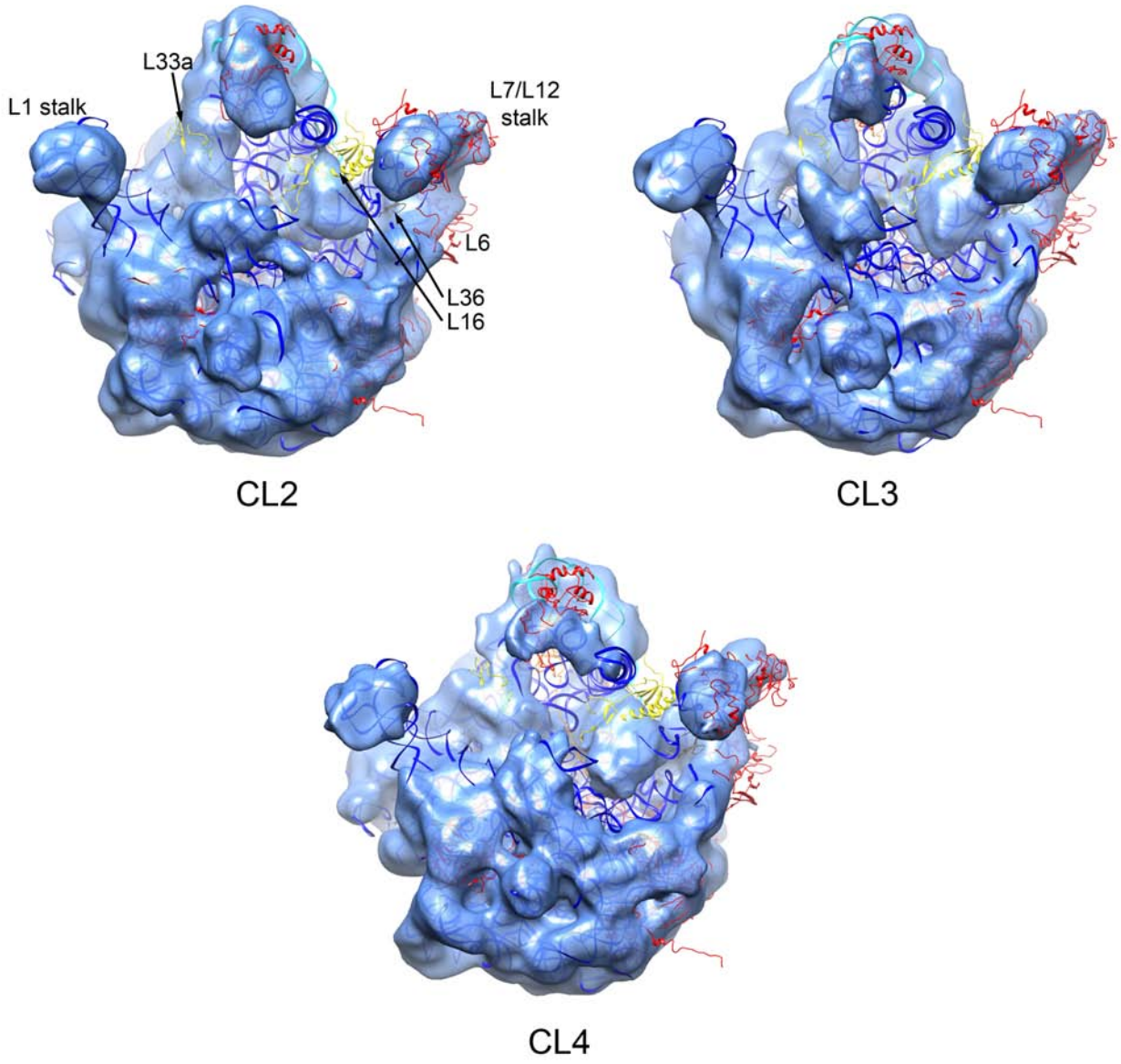

Supplementary Figure S6. Conformational subpopulations of the 45S particle. Cryo-EM maps representing three of the conformational subpopulations observed for the 45S particle. The map for class 1 (CL1) is shown in Figure 3B. The X-ray structure of the 50S subunit from *Thermus Thermophilus* (PDB ID 2Y11) is shown docked into the cryo-EM maps. The r-proteins for which a corresponding density was not observed in the cryo-EM map are labeled.

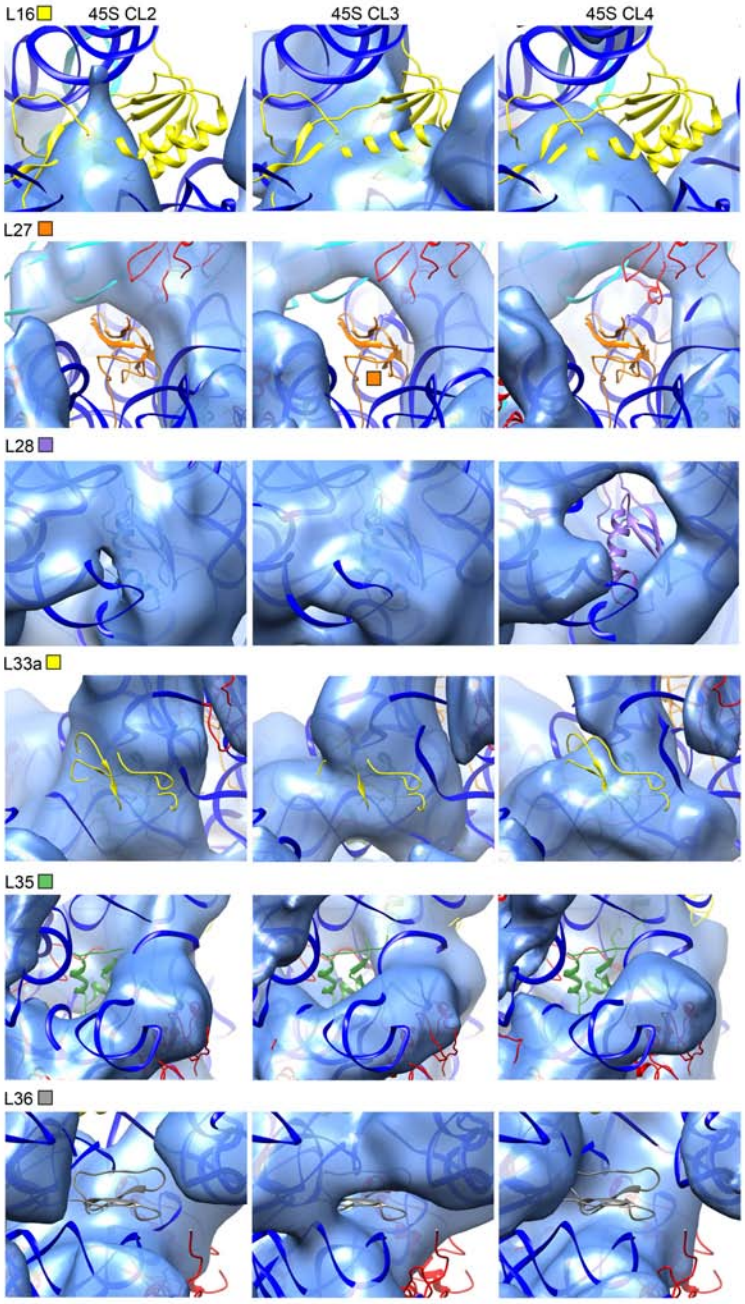

Supplementary Figure S7. Late binding r-proteins depleted or lacking in the 45S subunit. Close-up view of the densities representing the r-proteins found depleted or absent by qMS in the cryo-EM maps of the conformational subpopulations of the 45S particles. Each column shows the densities for these r-proteins in the cryo-EM map of one of the conformational subpopulations of the 45S particles. The X-ray structure of *Thermus Thermophilus* (PDB ID 2Y11) was docked into the cryo-EM maps to aid in the interpretation of the densities. A view of these densities in the conformational subpopulation 'CL1' is shown in Figure 4. Proteins are colored as indicated by the color code and the 23S rRNA is shown as a blue ribbon.

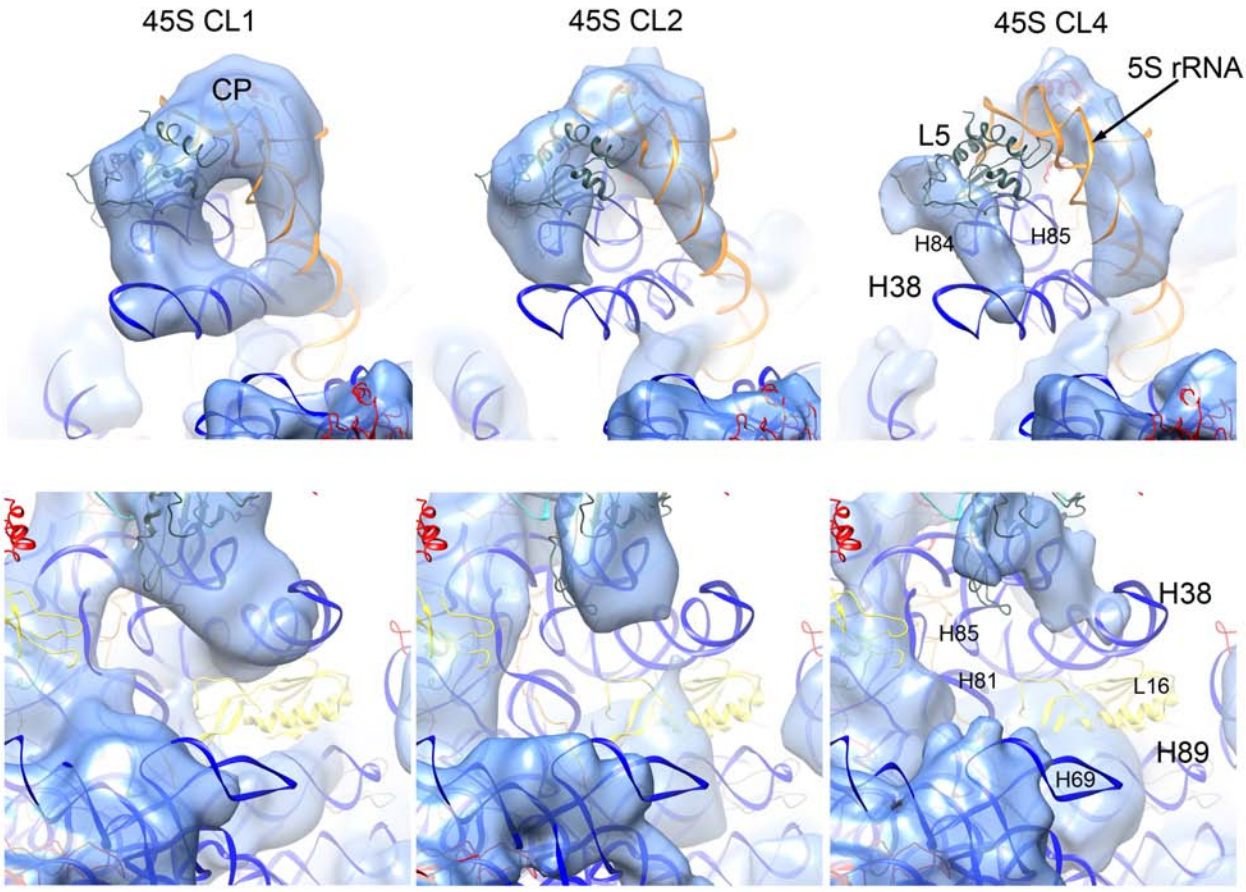

Supplementary Figure S8. Structural distortions of the central protuberance in the conformational subpopulations of the 45S particle. Side (from the L7/L12 stalk) (top panels) and front view (bottom panels) of the central protuberance (CP) of the cryo-EM maps of three conformational subpopulations of the 45S particle. Interpretation of the visible densities was done by docking the X-ray structure of the 50S subunit from *Thermus Thermophilus* (PDB ID 2Y11). Similar views of the map obtained for the conformational subpopulation 'CL3' is shown in Figure 5A.

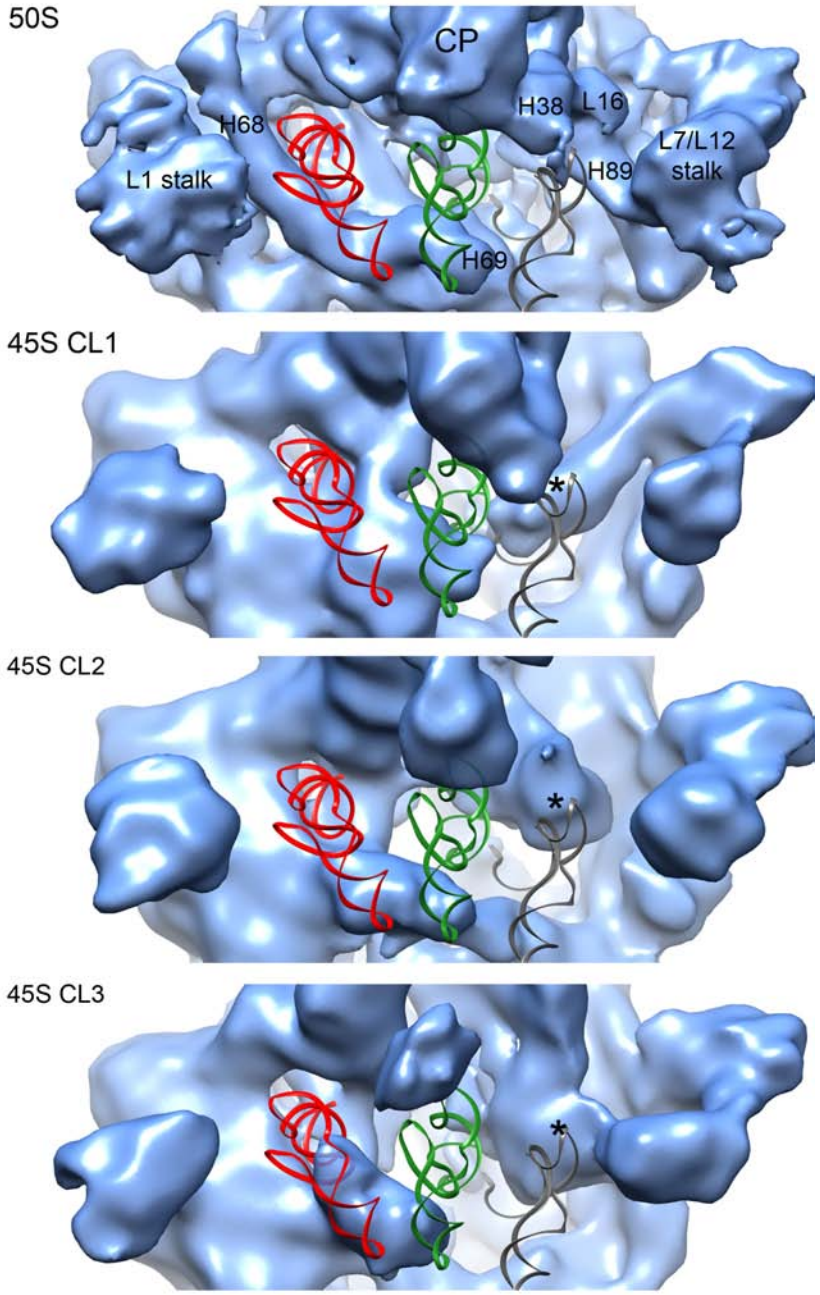

Supplementary Figure S9. Conformational differences in the tRNA binding sites in the 45S particle. The A, P and E t-RNA binding sites are compared between the cryo-EM maps of the mature 50S subunit and three of the conformational subpopulations of the 45S particle. An additional map representing a fourth subpopulation of the 45S particle is shown in Figure 5B. Three tRNA molecules from the X-ray structure of the 50S subunit from *Thermus Thermophilus* (PDB ID 1GIY) are shown docked into the A (grey), P (green) and E (red) sites of the cryo-EM map. Important landmarks and rRNA helices that showed distortions in the 45S particles are labeled. A prominent density occupying part of the A site is labeled with an asterisk.

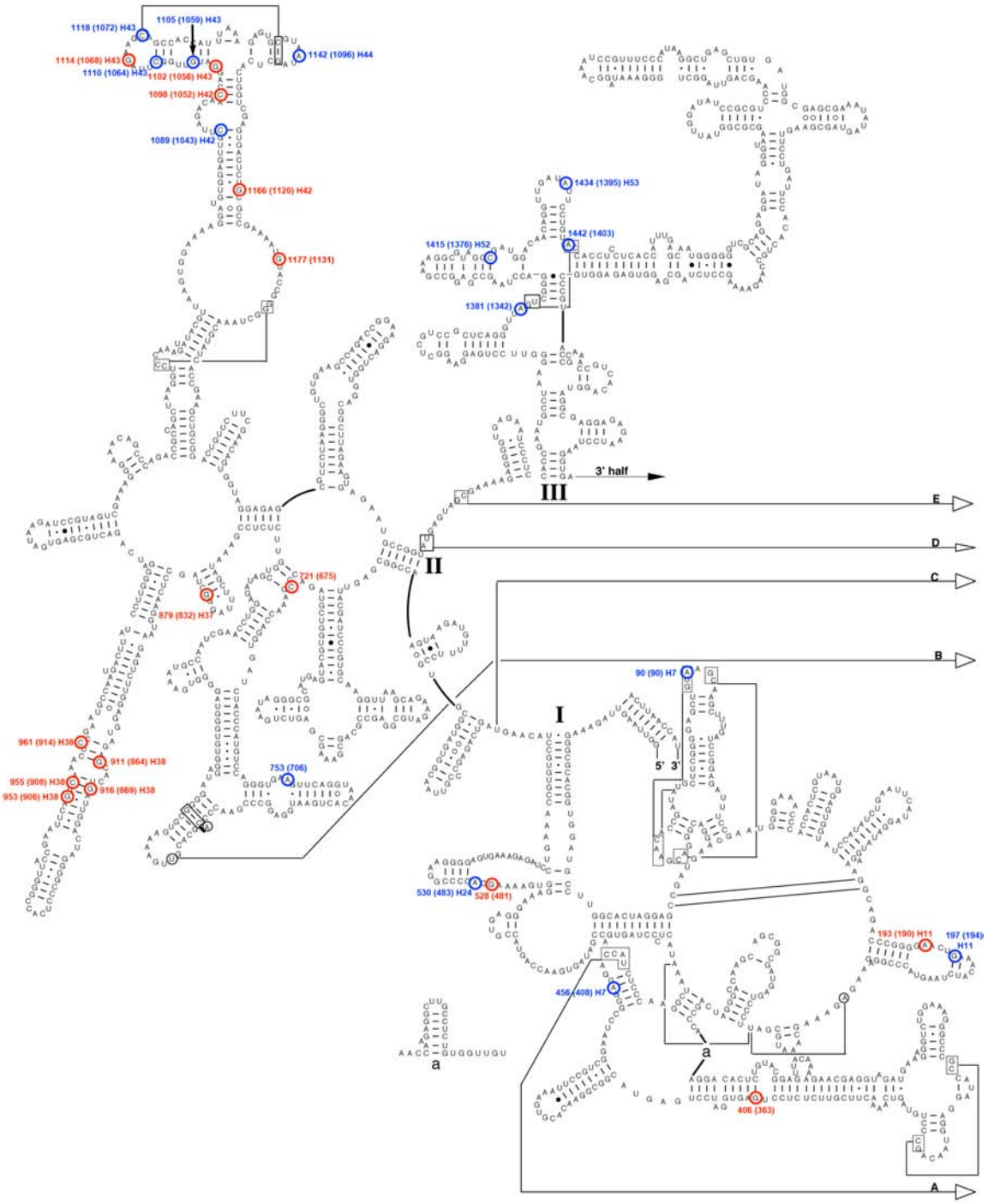

Supplementary Figure S10. Chemical modifications by DMS and kethoxal mapped in the secondary structure of the 23S rRNA (5′-half). Bases with increased (red) and decreased (blue) reactivity in the 45S particle compared to the mature 50S subunit are labeled in the secondary structure diagram of the 23S rRNA from *Bacillus subtilis*. Numbers in brackets correspond to *E. coli* numbering of the 23S rRNA).

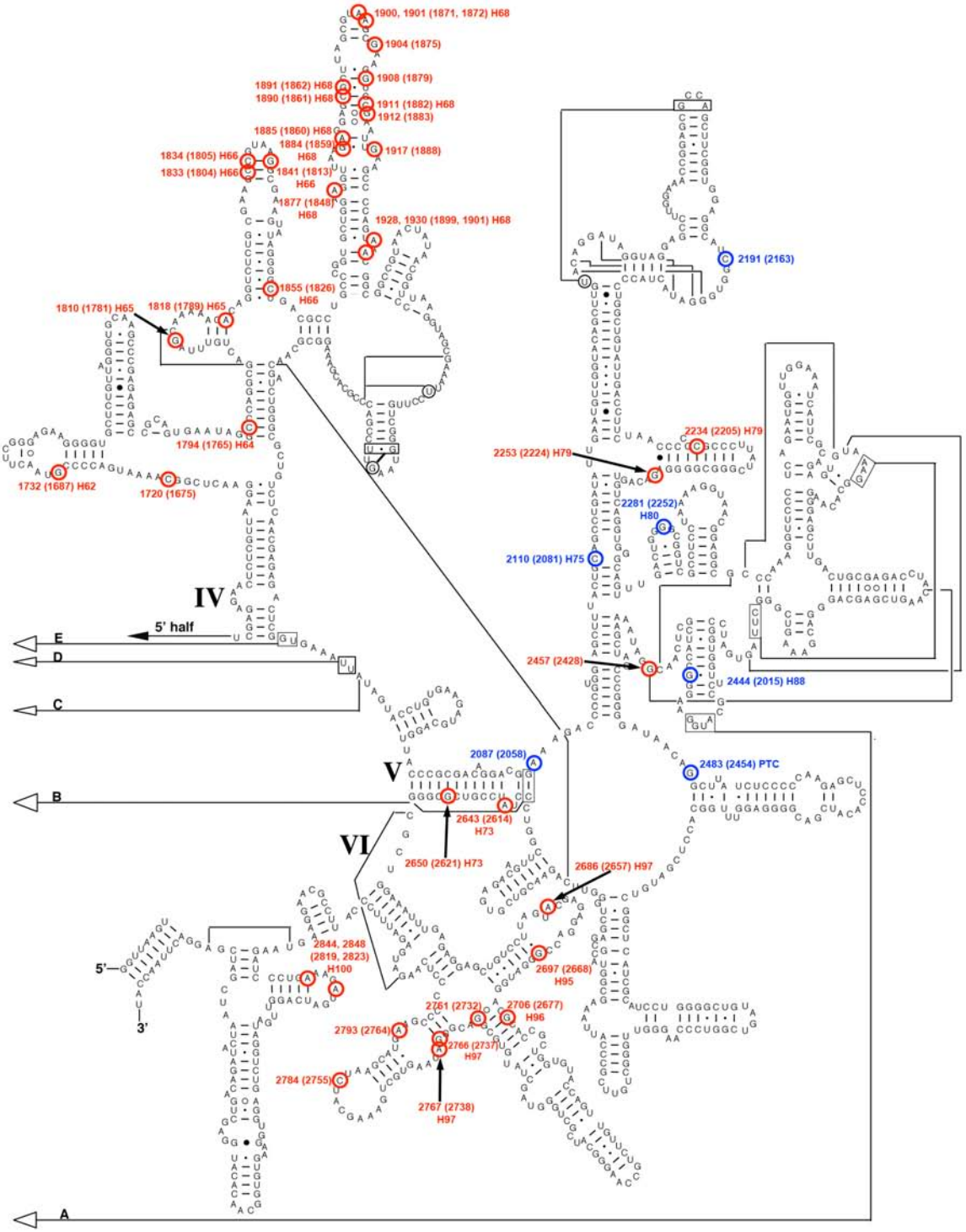

Supplementary Figure S11. Chemical modifications by DMS and kethoxal mapped in the secondary structure of the 23S rRNA (3′-half). Bases with increased (red) and decreased (blue) reactivity in the 45S particle compared to the mature 50S subunit are labeled in the secondary structure diagram of the 23S rRNA from *Bacillus subtilis*. Numbers in brackets correspond to *E. coli* numbering of the 23S rRNA).

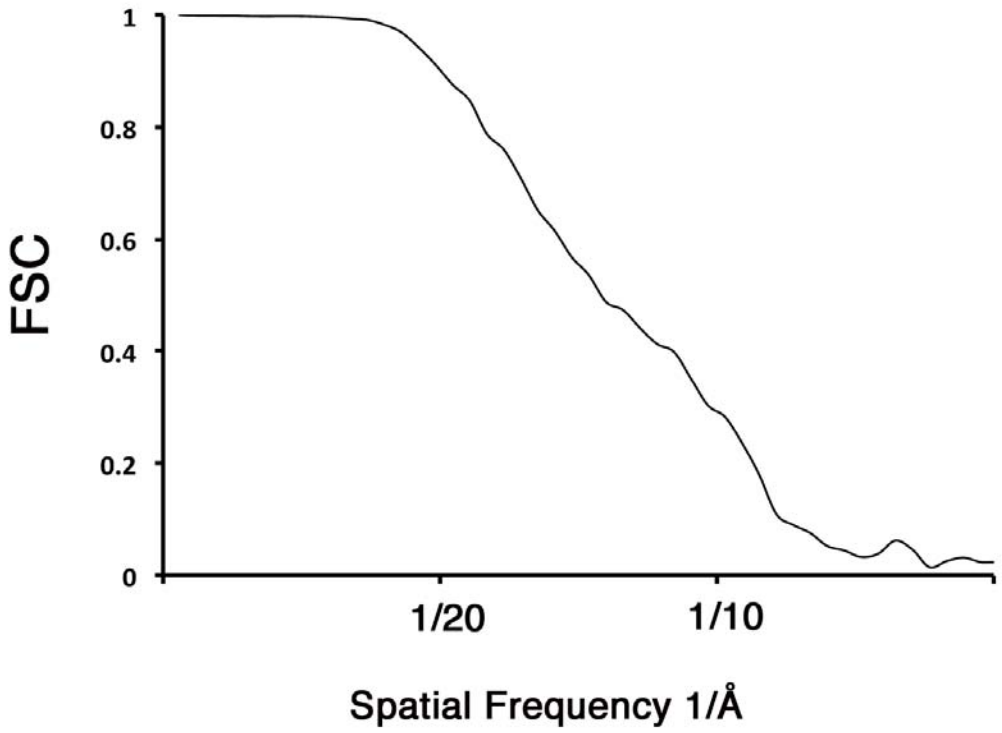

Supplementary Figure S12. Fourier Shell Correlation plots for resolution estimation of the L16-depleted 50S subunit reconstruction. Using the the FSC=0.5 criteria the estimated resolution for the 3D reconstruction of the L16-depleted 50S subunit was 13Å.

SUPPLEMENTARY TABLES

Primer	Modified base	Helix	*E. coli* base	Average fold modification*	Standard error	**p-value	Protein contacts	Domain
rp 357	193	H11	190	3.49	0.087	0.0202	None	
	90	H7	90	3.36	1.218	0.070	L23-Arg69	I
rp601	456	H22	408	4.25	1.729	0.041	None	
	530	H24	483	3.09	0.554	0.024	L24-Lys43,His44,Gln45,Pro54,Lys46	
rp846	753		706	6.12	2.128	0.006	L2-R13	
rp1055	961	H38	914	4.70	1.110	0.007	between L16 and L27 but no protein contacts	
	955	H38	908	3.60	0.850	0.010	L16-Asp70,Thr24,Phe68	
								II
rp1245	1142	H44	1096	3.78	1.063	0.042	None	
	1118	H43	1072	2.55	0.201	0.008	None	
	1110	H43	1064	2.91	0.324	0.012	L11-Gly90,Gly88	
	1098	H42	1052	2.47	0.223	0.009	None	
	1089	H42	1043	3.78	0.787	0.034	None	
rp1505	1442		1403	4.96	2.520	0.101	None	
	1434	H53	1395	4.93	0.914	0.013	None	III
	1415	H52	1376	2.61	0.389	0.024	None	
	1381		1342	3.18	0.794	0.042	L23-Asn59,Val58,Lys40	
rp1726	None							
rp1920	1855	H66	1826	2.27	0.095	0.003	L2-Gly221,Thr222,His231,Asn238,His242,	
	1834	H66	1805	3.22	0.401	0.013	L2-Asn45,Thr50,Arg51,Thr245	
	1818	H65	1789	3.31	0.420	0.012	L2-Val219,Arg220,Gly221,Pro217	
	1794	H64	1765	4.50	0.801	0.021	None	
	1720		1675	2.35	0.195	0.012	L3-His134	
rp2066	1930	H68	1901	11.03	2.917	0.019	L2-Gln250	IV
	1928	H68	1899	14.76	4.637	0.023	None	
	1911	H68	1882	9.55	2.989	0.028	None	
	1901	H68	1872	10.46	2.657	0.017	None	
	1900	H68	1871	7.90	1.990	0.022	None	
	1890	H68	1861	23.67	6.455	0.007	None	
	1885	H68	1860	33.42	9.088	0.005	None	
	1877	H68	1848	17.47	5.529	0.012	None	
rp2296	2234	H79	2205	6.31	2.084	0.036	L2-Gly148,Lys67	
	2191		2163	4.60	1.610	0.058	None	
	2110	H75	2081	4.84	1.827	0.067	L31(or L28 in *T. thermophilus*)-Ser15,Cys16,Ser17,Cys18,Gly19,Asn20, Val21, Met22,Lys23	V
	2087		2058	4.77	2.170	0.085	None	
rp2405	None							
rp2572	None							
rp2703	2643	H73	2614	3.26	0.721	0.011	L32-Ala1	
rp2913	2848	H100	2823	2.32	0.676	0.004	L3-Phe118,Gly117,Lys116, L17-Met1	
	2844	H100	2819	4.19	1.450	0.039	L17-Lys5,	
	2793		2764	2.68	1.094	0.071	None	IV
	2784		2755	4.16	0.649	0.012	L36-Arg19,Arg36	
	2767	H97	2738	3.25	0.390	0.001	None	
	2686	H95	2657	2.62	0.033	0.014	L6-Val91,Tyr93,Lys159,	

Supplementary Table 1. Chemical modifications of the 23S rRNA in the 45S particle using DMS. (*) Cells highlighted in red color depict increased modification in the 45S subunit, whereas blue color depicts increased modification in the 50S subunit. (**) A one sample two-tailed T-test was carried out on log transformed data and the p-value was calculated.

Primer	Modified base	Helix	*E. coli* base	Average fold modification*	Standard error	**p-value	Protein contacts	Domain
rp357	197	H11	194	3.09	0.404	0.015	None	
								I
rp601	528		481	2.40	0.513	0.023	L24-Lys43	
	406		363	7.51	1.659	0.012	None	
rP846	721		675	4.45	1.219	0.010	L4-Gln62,Gly71,Lys58,Ser72	
rp1055	953	H38	906	10.67	3.087	0.016	L16-Asp25,Arg66,Phe28,Phe68	
	916	H38	869	5.83	1.631	0.029	L16-Asp70,Met12,Phe9	
	911	H38	864	5.35	1.406	0.023	L16-His13	
	879	H37	832	3.84	1.194	0.061	None	II
rp1245	1177		1131	6.12	1.274	0.009	L13-His77,Lys85,Ile81	
	1166	H42	1120	5.73	0.679	0.014	None	
	1114	H43	1068	12.98	3.824	0.002	None	
	1105	H43	1059	4.81	0.844	0.004	L11-Gly130,Ser127,Met116,Lys112,Ala75,Arg133,Thr131,Asp115,Ile128	
	1102	H43	1056	3.52	0.609	0.001	none	
rp1505	None							
rp1726	None							III
rp1920	1841	H66	1813	2.44	0.236	0.013	L2-Arg42,Thr49,Thr50,Arg51	
	1833	H66	1804	3.94	0.987	0.030	L2-Arg51,Trp247,Lys254	
	1810	H65	1781	2.03	0.120	0.007	L34-Arg3	
	1732	H62	1687	3.63	0.478	0.010	None	
rp2066	1917	H68	1888	4.77	0.318	0.002	None	
	1912		1883	7.67	1.738	0.017	None	
	1908		1879	7.70	1.498	0.012	None	IV
	1904		1875	6.39	1.045	0.007	None	
	1891	H68	1862	7.03	1.997	0.036	None	
	1884	H68	1859	4.50	0.520	0.006	None	
	1841	H66	1813	4.84	0.874	0.015	L2-Asn43,Asn44,Asn45,Thr49,Thr50,Arg51	
rp2296	none							
rp2405								
	2281	H80	2252	57.78	21.199	0.007	None	
	2253	H79	2224	3.72	0.744	0.031	None	
rp2572	2483	PTC	2454	6.77	1.630	0.014	None	V
	2457		2428	2.60	0.153	0.004	L15-Leu61,Tyr58,	
	2444	H88	2415	5.18	0.088	<.001	L15-Thr67,Phe66,Gly65	
rp2703	None							
	2766	H97	2737	3.14	0.224	0.004	L13-Met92,Arg95	
rp2913	2761	H97	2732	4.37	1.330	0.046	None	VI
	2706	H96	2677	2.87	0.207	0.005	L3-Phe127,Trp125	
	2697	H95	2668	3.05	0.592	0.029	L6-Ser109	
	2650	H73	2621	3.19	0.078	<.001	L3-Arg124,Gly163,Gln164,Phe118	

Supplementary Table 2. Chemical modifications of the 23S rRNA in the 45S particle using kethoxal. (*) Cells highlighted in red color depict increased modification in the 45S subunit, whereas blue color depicts increased modification in the 50S subunit. (**) A one sample two-tailed T-test was carried out on log transformed data and the p-value was calculated.

Supplementary Table 3. Primers used in the DMS and Kethoxal chemical probing of the 23S rRNA in the mature 50S subunit and 45S particle assembly intermediate.

Oligonucleotide Name	Sequence
Bs_rp354	5'6-FAM CCTTTCCAGACCTCTTCATCTACC-3'
Bs_rp601	5'6-FAM ATCACCCGTTAACGGGCTCTGACT-3'
Bs_rp846	5'6-FAM CCAGGTTCGATTGGCATTTCACC-3'
Bs_rp1055	5'6-FAM TTGGGACCTTAGCTGGCGGTC-3'
Bs_rp1245	5'6-FAM CTTAGAACGCTCTCCTACCACTGT-3'
Bs_rp1505	5'6-FAM ATCCAATACCGCGCTTACCCTATC-3'
Bs_rp1726	5'6-FAM CATTTTGCCGAGTTCCTTAACGAGAG-3'
Bs_rp1920	5'6-FAM CTTCAATTCGCACCTTCGCTTACG-3'
Bs_rp2066	5'6-FAM TGCATCTTCACAGGTACTATAATTTCACC-3'
Bs_rp2296	5'6-FAM TTAGGAGGCGACCGCCCCAGTCA-3'
Bs_rp2405	5'6-FAM TCGTCCCTGCTCGACTTGTAGGT-3'
Bs_rp2572	5'6-FAM CTTGGGACCGACTACAGCCCC-3'
Bs_rp2703	5'6-FAM CCATCCCGGTCCTCTCGTAC-3'
Bs_rp2913	5'6-FAM ATCGATTAGTATCTGTCAGCTCCATGT-3'

All primers used in this study were 5′ 6-carboxyfluorescein (6-FAM) labeled.

The number in Oligos name indicate the starting base position in 23S rRNA (*rrnA* gene). “Bs “ stands for *Bacillus subtilis* and “rp” for reverse primer.

SUPPLEMENTARY REFERENCES

1. Chen, S.S. & Williamson, J.R. Characterization of the Ribosome Biogenesis Landscape in E. coli Using Quantitative Mass Spectrometry. *J Mol Biol* **425**, 767-79 (2013).
2. Chen, S.S., Sperling, E., Silverman, J.M., Davis, J.H. & Williamson, J.R. Measuring the dynamics of E. coli ribosome biogenesis using pulse-labeling and quantitative mass spectrometry. *Mol Biosyst* **8**, 3325-34 (2012).